Original Paper

EPR and voltammetric studies of iron-containing mixed alkali glasses with the basic composition $x\mathrm{Na_2O} \cdot (16-x)\mathrm{K_2O} \cdot 10\mathrm{CaO} \cdot 74\mathrm{SiO_2}$

Christian Rüssel

Otto-Schott-Institut für Glaschemie, Friedrich-Schiller-Universität Jena (Germany)

Mixed soda–potassium–lime glasses containing iron oxide in a concentration range of 0.1 to 2 mol% were studied by means of EPR spectroscopy and voltammetry. At low iron concentrations a one-step reduction of Fe^{III} to Fe^{II} was observed. The values of the standard reaction enthalpy, ΔH^0, and of the standard reaction entropy, ΔS^0, calculated from the temperature dependence of the standard potentials show maxima if sodium and potassium concentrations are approximately equal. EPR spectra of all glasses investigated show two paramagnetic signals at $g = 2.0$ and $g = 4.3$. The ratio of the peak intensities, $I_{2.0} / I_{4.3}$, increases with the square of the total iron concentration. Here, the intensity of the $g = 4.3$ peak increases with increasing Na_2O concentration; the behaviour of the mixed alkali glasses, however, cannot be explained as an additive effect.

EPR- und voltammetrische Untersuchungen an eisenhaltigen Mischalkaligläsern der Grundzusammensetzung $x\mathrm{Na_2O} \cdot (16-x)\mathrm{K_2O} \cdot 10\mathrm{CaO} \cdot 74\mathrm{SiO_2}$

Mischalkali–Kalksilicatgläser mit einem Stoffmengenanteil von 0,1 bis 2% Eisen wurden mit Hilfe der EPR-Spektroskopie und der Voltammetrie untersucht. Bei niedrigen Eisenkonzentrationen wurde eine einstufige Reduktion von Fe^{III} zu Fe^{II} beobachtet. Die aus der Temperaturabhängigkeit der Standardpotentiale ermittelten Werte für die Standard-Reaktionsenthalpie, ΔH^0, und die Standard-Reaktionsentropie, ΔS^0, wiesen jeweils ein Maximum auf, wenn etwa gleiche Natrium- und Kaliumkonzentrationen vorlagen. Die EPR-Spektren aller untersuchten Gläser zeigten zwei unterschiedliche paramagnetische Signale bei $g = 2{,}0$ und $g = 4{,}3$. Das Verhältnis dieser Peakintensitäten, $I_{2,0}/I_{4,3}$, steigt mit dem Quadrat der Gesamteisenkonzentration an. Hierbei nimmt die Intensität des Peaks bei $g = 4{,}3$ mit steigendem Na_2O-Gehalt zu, das Verhalten der Mischalkaligläser läßt sich jedoch nicht als additiver Effekt erklären.

1. Introduction

Various studies of the redox pair Fe^{II}/Fe^{III} with respect to its thermodynamics [1 to 17] and its incorporation [1, 18 to 31] within the glass melt have already been carried out. The most structural studies have been made using spectroscopic methods such as EPR [18 to 27], UVIS-NIR [28 and 29] or Mößbauer spectroscopy [30 and 31] at room temperature. Up to now, only a few studies have been published using spectroscopic methods at glass melt temperatures. The thermodynamics of the Fe^{II}/Fe^{III} redox pair has predominantly been studied either with the aid of equilibration experiments or using electrochemical measurements. Equilibration experiments have been carried out by equilibrating a glass melt with a gas atmosphere of a well-known oxygen fugacity at high temperature [1 to 9]. After some hours or days, the samples are quenched and analyzed physically or chemically. Electrochemical experiments are carried out in-situ directly in the glass melt at high temperatures. Using voltammetric measurements [10 to 17], current–potential curves are recorded from which thermodynamic data such as standard potentials, standard enthalpies and standard entropies as well as diffusion coefficients can be calculated. In principle, voltammetric methods may also provide information on the incorporation of the redox species into glass melts. In recent voltammetric studies of iron-containing alkali–lime–silica glasses, the type and concentration of alkali oxide were varied systematically and the influence on the thermodynamic behaviour was investigated [32]. EPR studies of the same iron-containing glasses were also carried out [33]. Systematic changes in the shape of the spectra were caused by both the iron concentration and the type of alkali cation present. By contrast, the alkali concentration did not have significant influence on the shape of the spectra within the investigated alkali concentration range of 10 to 25 mol%. Both the results of EPR spectroscopy and those of the voltammetric studies were explained by a structural model where Fe^{III} occurs as a tetrahedrally coordinated complex forming an ion pair with the alkali cation. At higher iron concentrations the changes in the EPR spectra and the occurrence of a two-step reduction process of Fe^{III} were explained by the formation of iron-containing clusters [32 and 33]. That means that a new model was introduced in which the thermodynamic and spectroscopic behaviour is no more explained by the traditional way where the iron occurs as ionic species or complex (e.g., FeO_4^{5-}) in a polar solvent (i.e., a dielectric continuum). It should be mentioned that using the continuum model both thermodynamic and spectroscopic behaviour could not be explained sufficiently with respect to the influence of the glass composition. In this

Received April 9, 1996.

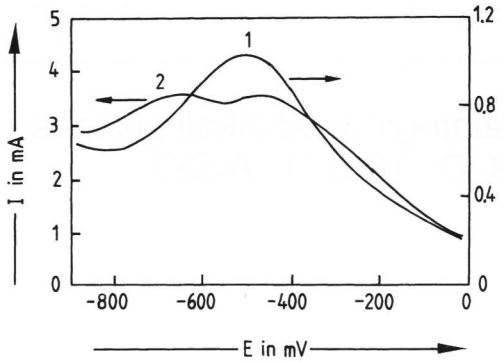

Figure 1. Square-wave voltammograms recorded in a glass melt with the basic composition (in mol%): $9.6Na_2O$, $6.4K_2O$, 10CaO, $74SiO_2$, doped with different quantities of Fe_2O_3; curve 1: 0.5, curve 2: 2.0. Temperature: 1200 °C, step time, τ: 10 ms, amplitude ΔE: 100 mV.

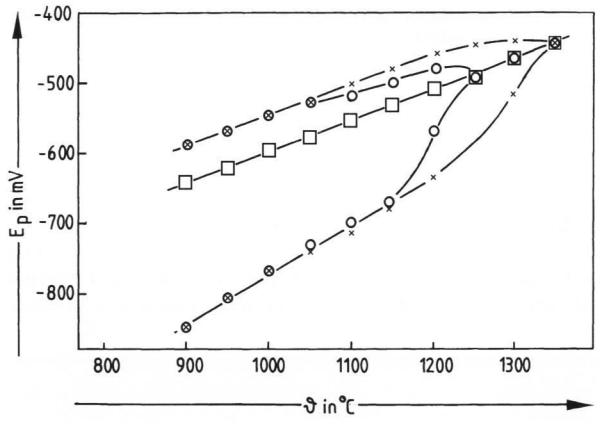

Figure 2. Peak potentials of voltammograms recorded in a glass melt with the basic composition (in mol%): $9.6Na_2O$, $6.4K_2O$, 10CaO, $74SiO_2$, doped with different quantities of Fe_2O_3, as a function of temperature; ×: 2.0, ○: 1.0, □: 0.5, 0.2, 0.1.

paper, a study of voltammetric as well as of EPR spectroscopic properties of iron oxide in mixed alkali glasses with the basic composition of $x Na_2O \cdot (16 - x)K_2O \cdot 10CaO \cdot 74SiO_2$ is reported.

2. Experimental

The experiments were carried out in glass melt and glasses with the basic composition (in mol%): $x Na_2O \cdot (16-x)K_2O \cdot 10CaO \cdot 74SiO_2$ (x = 0, 3.2, 6.4, 9.6, 12.8, 16); $20Na_2O \cdot 20CaO \cdot 60SiO_2$; $20Na_2O \cdot 10CaO \cdot 70SiO_2$ and $20Na_2O \cdot 80SiO_2$. The glasses were doped with 0.1 to 2 mol% Fe_2O_3. The glass melts were not equilibrated with air before the voltammetric measurements were carried out.

The EPR spectra were recorded in the x band (9.5 GHz) with an EPR spectrometer of Bruker Spektraspin, model 414 (Bruker, Brussels (Belgium)) at 25 °C. Voltammetric measurements were carried out in an electrically heated (SiC) furnace with a vertical alumina tube. In the middle of this tube, a platinum crucible containing the glass melt (around 60 g) was located. Three electrodes dipped into the glass melt: a platinum wire (diameter: 0.5 mm) as the working electrode, the counter electrode was a platinum plate (area: 2 cm^2) and the reference electrode was a zirconia probe with air as reference gas, in detail described in [12 and 13].

The dip-in length of the working electrode into the glass melt was adjusted by measuring the ac conductivity between working and counter electrode according to the procedure described in [13]. The electronics were self-constructed, the main part was a potentiostat connected to a microcomputer via analogue/digital and digital/analogue converter so that any potential–time dependence can be supplied and the current–potential curve recorded. The potential–time dependence of the square-wave voltammetry is a staircase ramp superimposed by a rectangular wave of comparably high frequency (5 to 500 s^{-1}) and amplitude (100 mV). The potential is held at 0 mV and then shifted to cathodic values in the range of −800 to −1000 mV. The current is measured at the end of every half-wave and then differentiated. The theory of the square-wave voltammetry is reported in full in [34 and 35]. Both, the experimental equipment and the procedure are in detail described in [12 and 13].

3. Results

In figure 1, square-wave voltammograms of a glass melt with the basic composition (in mol%): $9.6Na_2O \cdot 6.4K_2O \cdot 10CaO \cdot 74SiO_2$ doped with 0.5 and $2Fe_2O_3$ are shown. The voltammograms were recorded at 1200 °C using an amplitude of 100 mV and a step time of 10 ms. Curve 1 shows a voltammogram of the glass melt containing 0.5 mol% Fe_2O_3. The graph shows a peak at −500 mV which is attributed to the reduction of Fe^{3+} to Fe^{2+}. The shape of this peak is fairly similar to the theoretically calculated current–potential curve, however, notably influenced by background currents. The current increase at potentials lower than −800 mV is due to the decomposition of the glass matrix and the formation of elementary silicon or platinum silicide, while the increase at potentials above −50 mV is caused by the formation of gaseous oxygen. Curve 2 in figure 1 shows a voltammogram of the same glass melt doped with 2 mol% Fe_2O_3. By contrast to curve 1, the curve shows two distinct maxima at −460 and −640 mV.

Figure 2 presents the peak potentials measured as a function of temperature in a glass with the same basic compositions doped with 0.1, 0.2, 0.5, 1 and 2 mol% Fe_2O_3. At a concentration of 0.5 mol% and below, peak splitting does not occur. In this concentration range, the peak potentials depend, within the range investigated, linearly on temperature. By contrast, at an Fe_2O_3 concentration of 2 mol% peak splitting occurs at temperatures below 1350 °C. At an Fe_2O_3 concentration of 1 mol%, peak splitting is observed at temperatures below 1250 °C. Thus, at higher iron concentrations two branches occur which are attributed to two different peak potentials. They are approximately equal for 1 and

2 mol% Fe_2O_3 at temperatures below 1150 °C. Fairly similar behaviour was also observed at the other glass melt compositions investigated. At any of these compositions, peak splitting occurred at concentrations of 1 and 2 mol% Fe_2O_3, while at concentrations in the range of 0.1 to 0.5 mol% peak splitting was not observed. From the linear temperature dependence of the peak potentials, which are equal to the standard potentials, the standard enthalpy, ΔH^0, and the standard entropy, ΔS^0, can be calculated. Figure 3 shows these standard values for mixed alkali glasses as a function of the glass melt composition. The ΔH^0 values are in the range of 102 to 112 kJ mol^{-1}, while ΔS^0 possesses values between 33 and 39 J · K^{-1} mol^{-1}. Both graphs exhibit maxima at approximately equal concentrations of Na_2O and K_2O. It should be noted that the total concentration of alkali oxides was always 16 mol%. Although this effect is fairly small, it is clearly within the error limits of ± 1 kJ mol^{-1} for ΔH^0 and ± 2 J · K^{-1} mol^{-1} for ΔS^0.

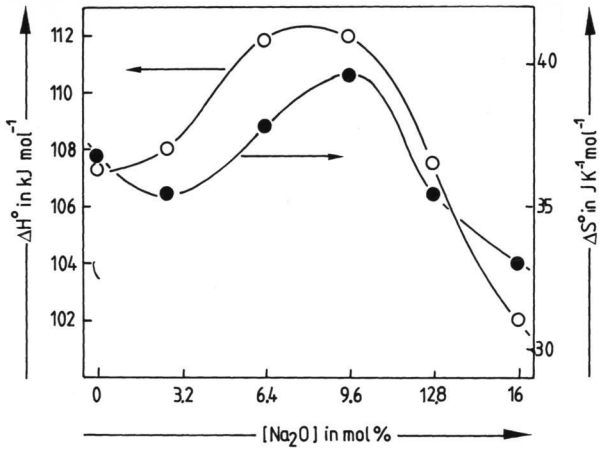

Figure 3. ΔH^0, ΔS^0 of the $[Fe^{2+}]/[Fe^{3+}]$ redox reaction as a function of the glass melt composition.

Figure 4 shows EPR spectra recorded in a glass melt with the basic composition (in mol%): $9.6Na_2O$, $6.4K_2O$, 10CaO and $74SiO_2$ doped with various quantities of Fe_2O_3. In each spectrum two different paramagnetic signals can be seen: a relatively sharp signal at around 0.15 V s m^{-2} which corresponds to a g value of 4.3, and a broad signal at around 0.33 V s m^{-2} attributed to $g = 2.0$. While for an Fe_2O_3 concentration of 0.1 mol%, the peak at $g = 2.0$ possesses only small peak-to-peak intensity, the peak at $g = 4.3$ is of fairly high intensity. With increasing quantity of Fe_2O_3 present, the intensities change notably and at concentrations of 1 and 2 mol% Fe_2O_3, the $g = 2.0$ peaks possess higher intensity than those at $g = 4.3$. In figure 5, the influence of the glass composition of mixed alkali glasses on the shape of the EPR spectra is shown. All glasses were doped with the same quantity of iron (0.5 mol%). While the EPR spectrum of the glass solely containing sodium, shows a comparably low intensity $g = 2.0$ peak, in the EPR spectrum of the solely potassium containing glass the $g = 2.0$ peak possesses nearly the same intensity as the $g = 4.3$ peak. The $g = 2.0$ peak intensities of the mixed alkali glasses are in between. Figure 6 shows the ratio of the peak intensities ($I_{2.0}/I_{4.3}$) as a function of the iron concentration. Since in former studies [33], a linear dependence of this relative intensity on the square of the total iron concentration was observed, the square root of the ratio ($I_{2.0}/I_{4.3}$) is drawn against the iron concentration. The relative intensity ($I_{2.0}/I_{4.3}$) for solely potassium and solely sodium containing glasses is illustrated by the lines 1 and 6, respectively. Also in the mixed alkali glasses, a linear dependence of the square root of the relative intensity on the total iron concentration is observed. The slope is highest for the glass containing solely potassium and then decreases with decreasing quantity of potassium present. The lowest slope is obtained if solely sodium containing glasses have been studied. Figure 7 shows the square root of the relative intensity ($I_{2.0}/I_{4.3}$) as a function of the total iron concentration for glasses with the basic composition (in mol%): $20Na_2O \cdot xCaO \cdot (80-x)SiO_2$ for $x = 0$, 10 and 20. Although the effect of the type of alkali cation on the relative intensities is much stronger, the quantity of calcium oxide present also influences the relative intensities notably. The slope decreases with the quantity of lime present by around 20 %.

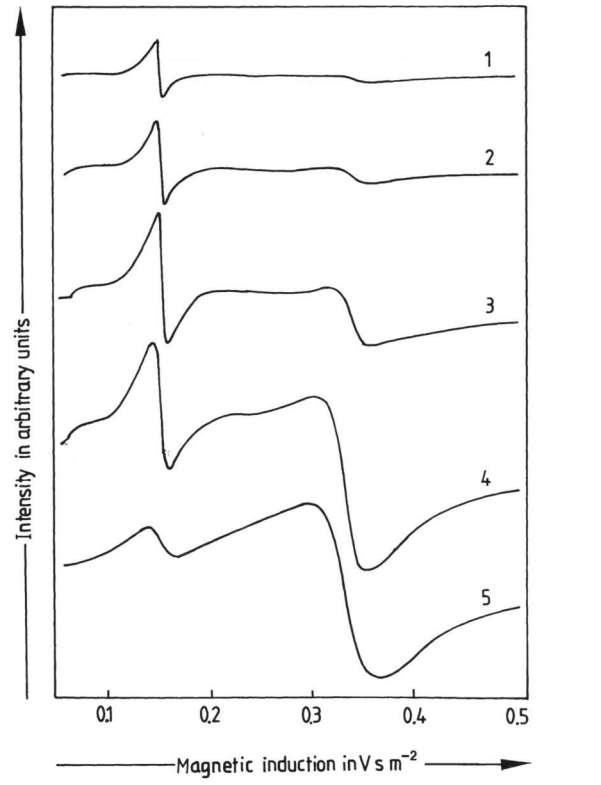

Figure 4. EPR spectra recorded in a glass melt with the basic composition (in mol%): $9.6Na_2O$, $6.4K_2O$, $74SiO_2$ as a function of the iron concentration (Fe_2O_3 in mol%); curve 1: 0.1, curve 2: 0.2, curve 3: 0.5, curve 4: 1.0, curve 5: 2.0.

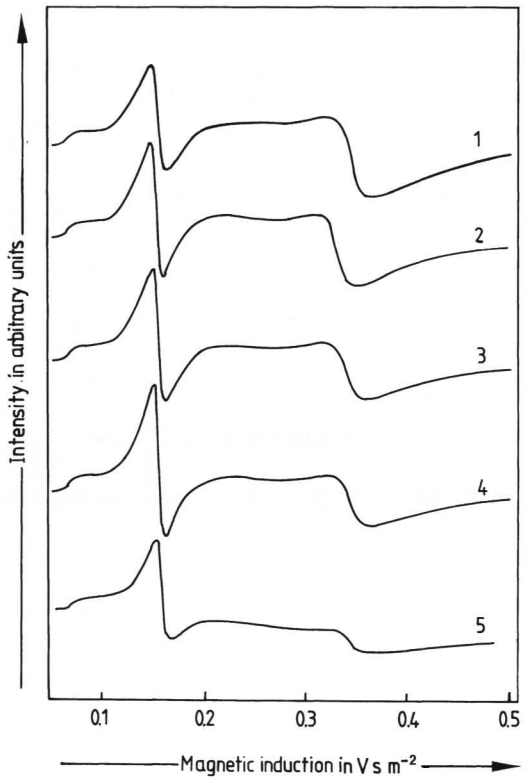

Figure 5. EPR spectra of glasses with the basic composition (in mol%): $x\mathrm{Na_2O} \cdot (16-x)\mathrm{K_2O} \cdot 10\mathrm{CaO} \cdot 74\mathrm{SiO_2}$, doped with $0.5\mathrm{Fe_2O_3}$; curve 1: $x = 0$, curve 2: $x = 3.2$, curve 3: $x = 6.4$, curve 4: $x = 9.6$, curve 5: $x = 16.0$.

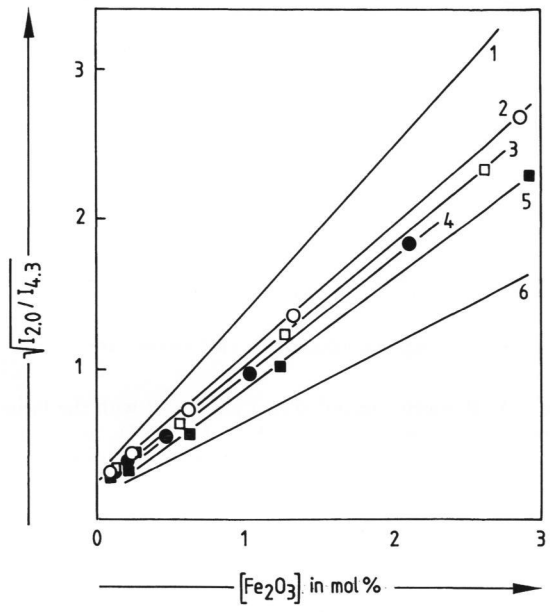

Figure 6. Square root of the ratio of the peak intensities at $g = 2.0$ and $g = 4.3$, $I_{2.0}/I_{4.3}$, of glasses with the basic composition (in mol%): $x\mathrm{Na_2O} \cdot (16-x)\mathrm{K_2O} \cdot 10\mathrm{CaO} \cdot 74\mathrm{SiO_2}$ as a function of the quantity of $\mathrm{Fe_2O_3}$ added; line 1: $x = 0$ [33], line 2: $x = 3.2$, line 3: $x = 6.4$, line 4: $x = 9.6$, line 5: $x = 12.8$, line 6: $x = 16.0$ [33].

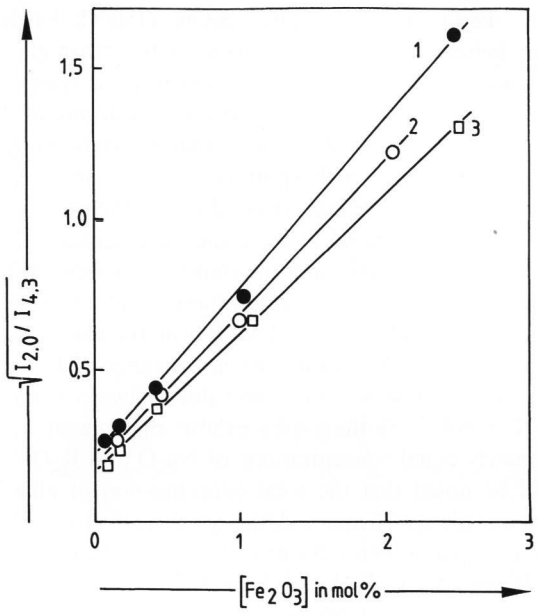

Figure 7. Square root of the ratio of the peak intensities at $g = 2.0$ and $g = 4.3$, $I_{2.0}/I_{4.3}$, of glasses with the basic composition (in mol%): $20\mathrm{Na_2O} \cdot x\mathrm{CaO} \cdot (80-x)\mathrm{SiO_2}$ as a function of the quantity of $\mathrm{Fe_2O_3}$ added; line 1: $x = 0$, line 2: $x = 10.0$, line 3: $x = 20.0$.

4. Discussion

The linear dependences of the standard potentials on temperature at low iron concentration allow the calculation of the standard enthalpy, ΔH^0, and the standard entropy, ΔS^0. The dependence of these standard values as shown in figure 3 cannot be described as a function of the optical basicity of the melt. This basicity, which can be calculated from the glass composition according to Duffy [36], increases linearly with the potassium content from a value of 0.57 for the soda–lime glass to 0.59 for the potassium–lime glass, while both ΔH^0 and ΔS^0 exhibit maxima as shown in figure 3. In [32], ΔH^0 and ΔS^0 values are given as a function of the alkali concentration of soda–lime and potassium–lime–silica glasses. But also in these cases, the thermodynamic values did not montonously depend on basicity. At high iron concentrations peak splitting, i.e. two peaks at two different standard potentials, is observed, which must be attributable to two different electroactive species. This behaviour cannot be explained by the occurrence of Fe^{III} in octahedral and tetrahedral coordination, because this should lead to very different mobilities and hence diffusion coefficients. Therefore, for that case, very different peak currents for the reduction of these differently coordinated iron species should be observed. However, in the experimentally measured voltammograms the peak currents of these two steps are approximately equal and the ratio of the peak currents neither depends on the $\mathrm{Fe_2O_3}$ concentration (if >1 mol%) nor on the temperature. It should be noted that the same behaviour has also been

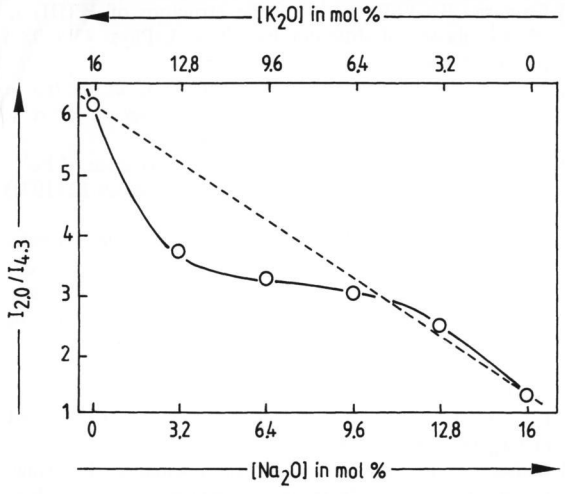

Figure 8. Ratio of the peak intensities at $g = 2.0$ and $g = 4.3$, $I_{2.0}/I_{4.3}$, of mixed alkali glasses doped with 2 mol% Fe_2O_3.

observed for soda–lime and potassium–lime–silica glasses, and obviously, this fact does not change notably if mixed alkali glasses are investigated.

The shape of the EPR spectra strongly depends on the iron concentration and the empirically found relation [33, equation (4)] is also valid

$$A \cdot C_{Fe^{III}} = \sqrt{I_{2.0}/I_{4.3}} \qquad (1)$$

for mixed alkali glasses. In [33], it was pointed out that the slope A (see figure 6) is not a function of the optical basicity, because A for lithium, sodium, potassium and cesium lime glasses did not depend on the quantity of alkali (for $[M_2O] > 10$ mol%), but solely on the type of alkali present. This was interpreted as a stabilization of the structure causing the $g = 4.3$ peak predominantly by small alkali cations and the structural model suggested was: Fe^{III} is tetrahedrally coordinated with oxygen forming Fe–O–Si groups and therefore, iron possesses a formal charge of -1. To achieve electroneutrality, the participation of alkali or in principle also of calcium cations is necessary. To obtain a g value of 4.3, the C_{2V} symmetry of the paramagnetic species is necessary and hence, the alkali cation is assumed to be coordinated with two oxygens of the Fe^{III} tetrahedron. If this cation is small, the stabilization of this structure is more advantageous, due to higher electrostatic forces and to bond angles closer to that of 90° required for an octahedral coordination of the alkali cation. If more than one type of alkali cation is present, the situation is more complicated, because the C_{2V} symmetry of tetrahedrally coordinated Fe^{III} can be achieved in the present case by sodium, potassium and in principle also by calcium. Figure 8 illustrates the relative intensities ($I_{2.0}/I_{4.3}$) as a function of the sodium content of mixed alkali glasses. If the probability of the sodium and the potassium ions to form the C_{2V} structure were equal, then the dependence on the sodium concentration described by the straight full line in figure 8 would result. The effect of the substitution of one fifth the quantity of sodium for potassium on the relative intensities, however, is much stronger. At a sodium concentration of 3.2 mol%, the relative intensity $I_{2.0}/I_{4.3}$ is only 60 % of that value which corresponds to the full line in figure 8. Therefore, it can be concluded that predominantly sodium occurs within the C_{2V} structure formed in the mixed alkali glass. However, as pointed out in [33], in soda–lime glasses, $I_{2.0}/I_{4.3}$ does not depend on the Na_2O concentration within the range of 10 to 25 mol%, and hence $I_{2.0}/I_{4.3}$ is lower in a glass containing 10 mol% sodium oxide than in a glass containing 9.6 or 12.8 mol% Na_2O and additionally K_2O. Thus, potassium oxide added to a soda–lime–silica glass destabilizes the C_{2V} structure and promotes the formation of clusters. This cannot be explained by either the structural model described above nor by the EPR behaviour of soda–lime and potassium–lime–silica glasses. Therefore, it has to be considered as a non-additive effect and hence a true mixed alkali effect.

The dependence of $I_{2.0}/I_{4.3}$ on the lime concentration shown in figure 7, although comparably small, is clearly significant and points out that higher quantities of lime contribute to the stabilization of the C_{2V} structure. The ratio $I_{2.0}/I_{4.3}$ is highest in absence of CaO and lowest at a concentration of 20 mol% CaO.

5. Conclusion

This paper describes the EPR spectroscopic as well as the voltammetric behaviour of soda–potassium–lime–silica glasses. Two non-additive effects are observed: ΔH^0 and ΔS^0 possess maximum values if potassium and sodium concentrations are approximately equal. The second effect is the stabilization of the C_{2V} symmetry of tetrahedrally coordinated Fe^{III}. Here not only sodium but also potassium and calcium influence the stabilization. Both effects are considered to be true mixed alkali effects which cannot be explained by a superimposition of effects observed in glasses containing solely one type of alkali. By contrast to the well-known mixed alkali effects concerning electric conductivity and diffusivity neither of the effects described above is a kinetic effect.

*

This work was funded by the Deutsche Forschungsgemeinschaft (DFG), Bonn-Bad Godesberg (Germany).

6. References

[1] Hirashima, H.; Yoshida, T.; Brückner, R.: Redox equilibria and constitution of polyvalent ions in oxide melts and glasses. Glastech. Ber. **61** (1988) no. 10, p. 283–292.

[2] Paul, A.; Douglas, R. W.: Ferrous–ferric equilibrium in binary alkali silicate glasses. Phys. Chem. Glasses **6** (1965) no. 6, p. 207–211.

[3] Lauer, H. V. jr.; Morris, R. V.: Redox equilibria of multivalent ions in silicate glasses. J. Am. Ceram. Soc. **60** (1977) no. 9–10, p. 443–451.

[4] Paul, A.: Effect of thermal stabilization on redox equilibria and colour of glass. J. Non-Cryst. Solids **71** (1985) p. 269–278.
[5] Majumdar, R.; Lahiri, D.: Equilibrium studies of Fe in alkali phosphate glasses. J. Am. Ceram. Soc. **58** (1975) no. 3–4, p. 99–101.
[6] Jeddeloh, G.: The redox equilibrium in silicate melts. Phys. Chem. Glasses **25** (1984) no. 6, p. 163–164.
[7] Yoshida, T.; Okada, Y.; Hirashima, H.: The effect of iron oxide concentration on redox equilibrium of the melts of $FeO-Fe_2O_3-RP_2O_6$ system (R ≡ Mg, Ca, Ba) with gas phase. (Orig. Jpn. with Engl. Abstr.) J. Ceram. Soc. Jpn. **81** (1973) no. 7, p. 281–289.
[8] Schreiber, H. D.; Kozak, S. J.; Merkel, R. C. et al.: Redox equilibria and kinetics of iron in a borosilicate glass-forming melt. J. Non-Cryst. Solids **84** (1986) p. 186–195.
[9] Schreiber H. D.; Minnix, L. M.; Balazs, G. B. et al.: The chemistry of uranium in borosilicate glasses. Pt. 4. The ferric–ferrous couple as a potential redox buffer for the uranium redox state distribution against oxidising agents in a borosilicate melt. Phys. Chem. Glasses **25** (1984) no. 1, p. 1–10.
[10] Takahashi, K.; Miura, Y.: Electrochemical behavior of glass melts. J. Non-Cryst. Solids **95 & 96** (1987) Pt. 1, p. 119–130.
[11] Takahashi, K.; Miura, Y.: Electrochemical studies on redox behavior of metallic ions in molten oxide glasses. Glastech. Ber. **56K** (1983) Bd. 2, p. 928–933.
[12] Freude, E.; Rüssel, C.: Voltammetric methods for determining polyvalent ions in glass melts. Glastech. Ber. **60** (1987) no. 6, p. 202–204.
[13] Montel, C.; Rüssel, C.; Freude, E.: Square-wave voltammetry as a method for the quantitative in-situ determination of polyvalent elements in molten glass. Glastech. Ber. **61** (1988) no. 3, p. 59–63.
[14] Rüssel, C.; Freude, E.: Voltammetric studies of the redox behaviour of various multivalent ions in soda–lime–silica glass melts. Phys. Chem. Glasses **30** (1989) no. 2, p. 62–68.
[15] Rüssel, C.; Freude, E.: Voltammetric studies in a soda–lime–silica glass melt containing two different polyvalent ions. Glastech. Ber. **63** (1990) no. 6, p. 149–153.
[16] Freude, E.; Rüssel, C.: Iron in glass melts – A voltammetric investigation. Glastech. Ber. **63** (1990) no. 7, p. 193–197.
[17] Maric, M.; Brungs, M. P.; Skyllas-Kazacos, M.: Voltammetric studies of the Fe(III) and Fe(II) species in molten sodium disilicate glass. Phys. Chem. Glasses **30** (1989) no. 1, p. 5–11.
[18] Sands, R. H.: Paramagnetic resonance absorption in glass. Phys. Rev. **99** (1955) p. 1222.
[19] Griscom, D. L.: Electron spin resonance. In: Uhlmann, D. R.; Kreidl, N. J. (eds.): Glass Science and Technology. Vol. 4B. Advances in structural analysis. Boston (et al.): Academic Press, 1990. p. 151–251.
[20] Castner, T.; Newell, G. S.; Holton, W. C. et al.: Note on the paramagnetic resonance of iron in glasses. J. Chem. Phys. **32** (1960) p. 668–673.
[21] Camara, B.: ESR study of the structure of Fe(III) in silicate glasses of different basicities. J. Phys. **43** (1982) p. C9/165-C9/168.
[22] Montenero, A.; Friggeri, M.; Giorno, D. C. et al.: Iron–soda–silica glasses: Preparation, properties, structure. J. Non-Cryst. Solids **84** (1986) p. 45–60.
[23] Loveridge, D.; Parke, S.: Electron spin resonance of Fe^{3+}, Mn^{2+}, and Cr^{3+} in glasses. Phys. Chem. Glasses **12** (1971) no. 1, p. 19–27.
[24] Camara, B.; Schaeffer, H. A.: Untersuchung der Farbelemente Chrom, Kobalt und Eisen in Silicatgläsern, Glasurfritten und Farbkörpern. T.l. Spektroskopische Charakterisierung (A study of chrome, cobalt and iron as coloring elements in silicate glasses, glaze frits and ceramic stains. Pt. 1. Spectroscopic characterization). (In German and Engl.) cfi/Ber. DKG **58** (1981) no. 7, p. 519–524.
[25] Camara, B.: Einbau von Eisen in Glas. Glastech. Ber. **51** (1978) no. 5, p. 87–95.
[26] Galas, C.: Electron paramagnetic resonance. In: Hawthorne, F. C. (ed.): Spectroscopic methods in mineralogy and geology. Washington: Mineralogical Society of America, 1988. p. 513–572. (Reviews in Mineralogy. Vol. 18.)
[27] Gravanis, G.; Rüssel, C.: Redox reactions in Fe_2O_3, As_2O_5 and Mn_2O_3 doped soda-lime-silica glasses during cooling – A high-temperature ESR investigation. Glastech. Ber. **62** (1989) no. 10, p. 345–350.
[28] Steele, F. N.; Douglas, R. W.: Some observations on the absorption of iron in silicate and borate glasses. Phys. Chem. Glasses **6** (1965) no. 6, p. 246–252.
[29] Traverse, J.-P.; Toganidis, T.; Adès, C.: Spectrophotometric analysis of ferrous, ferric and total iron content in soda–lime–silica glass. Glastech. Ber. **65** (1992) no. 8, p. 201–206.
[30] Kurkjian, C. R.; Sigety, E. A.: Mößbauer studies in inorganic glasses. In: VII^e Congrès International du Verre, Bruxelles 1965. C. r. Charleroi: Institut National du Verre, 1965. I.3.3., p. 39.1–39.8.
[31] Tomandl, G.; Frischat, G. H.; Oel, H. J.: Mößbauer-Effekt an Eisen-Alkali-Silicat-Gläsern. Glastech. Ber. **40** (1967) no. 8, p. 293–298.
[32] Rüssel, C.: Iron oxide-doped alkali–lime–silica glasses. Pt. 2. Voltammetric studies. Glastech. Ber. **66** (1993) no. 4, p. 93–99.
[33] Rüssel, C.: Iron oxide-doped alkali–lime–silica glasses. Pt. 1. EPR investigations. Glastech. Ber. **66** (1993) no. 3, p. 68–75.
[34] Osteryoung, J. G.; O'Dea, J. J.: Square-wave voltammetry. In: Bard, A. J. (ed.): Electroanalytical chemistry. Vol. 14. New York, Basel: Dekker, 1986. p. 209–308.
[35] Barker, G. C.: Square-wave polarography and some related techniques. Anal. Chim. Acta **18** (1958) p. 118–131.
[36] Duffy, J. A.; Ingram, M. D.: An interpretation of glass chemistry in terms of the optical basicity concept. J. Non-Cryst. Solids **21** (1976) p. 373–410.

0197P003

Address of the author:
C. Rüssel
Otto-Schott-Institut für Glaschemie
Friedrich-Schiller-Universität
Fraunhoferstraße 6, D-07743 Jena